

Fundamental Analysis on substrate distortion induced by Wire Arc Additive Manufacturing using experiment and nonlinear FEM with simplified bead model

Keval P Prajadhiana¹, Yupiter HP Manurung¹, Zaidi Minggu¹, Fetisia HS Pengadau¹, Hui Leng Choo²
Marcel Graf³, Andre Haelsig³, Tom-Eric Adams³, Dendi P Ishak⁴

¹Faculty of Mechanical Engineering, Universiti Teknologi MARA, Malaysia

²Taylor's University, Malaysia

³Chemnitz University of Technology, Germany

⁴Department of Industrial Engineering, University of Indonesia, Indonesia

*Corresponding author E-mail: yupiter.manurung@salam.edu.my

Abstract

In this fundamental research, Wire Arc Additive Manufacturing (WAAM) was investigated experimentally with regard to process parameter, bead quality and bead model development. A series of experiment was conducted by using robotic welding system ABB IRB 2400/16 and KEMMPI Pro Evolution ProMIG 540MXE with $\varnothing 1.2\text{mm}$ filler wire (AWS A5.28 : ER80S-Ni1) and shielding gas (80% AR/ 20% CO₂) on 6mm-thick substrate of Low Carbon Steel S235. Based on the experimental result, WAAM geometry is modelled using simplified bead shape following rectangular form under consideration of diluted material. The simulation was carried out by utilizing thermo-mechanical Finite Element Method (FEM) under consideration of non-linear isotropic hardening using commercial FEM software MSC Marc/Mentat. The plasticity model of Low carbon steel and high strength steel also considered under material properties option featured in software database. As comparison, similar material properties from previous researches were implemented into simulation to ensure a realistic resemblance. The analysis of substrate distortion is carried out by utilizing the coordinate measurement machine (CMM) pointed on various locations of substrate with 10 layers and 1 string WAAM. Based on the results between experiment and simulation, it is found out that FEM result with simplified bead model and equivalent plasticity model exhibits a good agreement which falls under the acceptable range of error.

Keywords: WAAM, FEM, Bead Model, Distortion, Isotropic Hardening

1. Introduction

Today, Additive Manufacturing (AM) widely used on producing a build-up products by means of layer by layer deposition instead employing the traditional machining of raw materials. Additive manufacturing serves as alternative on fabricating components which are made by titanium, aluminium alloys and other expensive materials because high value of the buy-to-fly ratio. Many techniques have been developed for manufacturing metal structures in AM, such as selective laser sintering, direct metal deposition, electron beam melting, shape deposition manufacturing, and wire and arc additive manufacturing (WAAM) [1].

The Additive Manufacturing which involves Gas Metal Arc Welding as its base operation is called Wire Arc Additive Manufacturing (WAAM). This process also executed by means of layer by layer strategy which able to create a large part with higher deposition rate compared to other AM based process [2]. In WAAM, a filler material is usually melted using electric arc which established between the consumable wire electrode and the top surface of deposited layers, while the component formed by depositions experiences the heating and cooling with moving heat source model [3].

Arc-welding-based additive manufacturing is one of the wire feed AM technologies, and uses either the gas metal arc welding process

(GMAW) or the gas tungsten arc welding process (GTAW) [4]. A notable benefit of WAAM are dominantly save cost by means of reductions in material required along with reductions in lead time, thus optimize the overall process design [5]. Two important aspects of depositions pattern of WAAM consists of the reluctant deformed state of the final part along with the efficiency in deposition. Deposition efficiency means that both avoidance of deposition failures and best toolpath generation are qualified to build a part which has the dimension as close as possible to the final shape of desired geometry [6].

The high deposition rate of WAAM process allows the creation of complex metal component in a flexible manner with high velocity, however, at some cases such flexibility results in large thermal gradients in work piece, causing the emergence of distortion. The involvement of Finite Element Method (FEM) is an essential aspect on prediction the level of distortion and residual stress within the WAAM component, which allows the optimization of planning prior to the actual WAAM process which if executed in correct term, should avoid costly trials [7]. Prior the rise of FE method, a traditional method such as parameter trial and error is often executed, of which said procedure could leads into high usage of material and labour which is not cost efficient along with the best welding quality which could be unobtainable [8].

Finite Element Analysis of WAAM is originated from multi-pass welding which has been collected from previous researches [9] The

inclusion of transformation strains caused by solid-state phase transformation presenting steels has been shown to be critical in weld modelling due to the fact that transformation strains influence bulk distortion and residual stress of work pieces, with lower martensite-start temperature yielding reduced levels of a distortion [10,11].

2. Experimental Set-up and Procedures

A series of comprehensive WAAM experiment was done by utilizing the facility installed on the Advanced Manufacturing lab of Faculty Mechanical Engineering, UiTM Shah Alam. Sample of commercially sourced low Carbon steel plate with dimensions 200 mm x 50 mm x 6 mm were assigned as the substrate of which weld beads were deposited using HSLA ER80S-Ni1 wire with a diameter of 1.2mm. The chemical composition for both materials is exhibited in table 1.

Table 1: Chemical compositions of S235 (top) and ER80S-NI (below)

C	Si	S	Cr	Cu	Mn	P	Ni	Mo
0.22	0.05	0.05	-	-	1.60	0.05	-	-
C	Si	S	Cr	Cu	Mn	P	Ni	Mo
0.07	0.4	0.02	0.15	0.35	1.0	0.02	0.80	0.15
-	-	-	-	-	-	-	-	-
0.12	0.80	-	-	-	1.50	-	1.10	-

The robotic welding machine which utilized for the whole experiment process is ABB IRB 2400/16 along with its power source KEMMPI Pro Evolution ProMIG 540MXE, both of equipment are displayed by Figure 1 below. Common parameters which present in GMAW welding process such as voltage (V), arc current (I), travel speed (TS) and wire feed speed ratio (WFSR) were accustomed according to characterization of deposited weld beads. The component of experimental result would later be cut, grinded, polished and etched prior taken into microscope analysis. The macrographs displayed here features a width and length multiplied as square feet along with it dilution that affects the surrounding beads. An actual number of width and length displayed by macrograph will be implemented as bead dimension in FEM simulation in order to keep the similarities between experimental and FEM. Figure 2 exhibits the bead modelling on FEM based on macrograph displayed from experiment result.

The dilution which occurs on the first layer and substrate is taken into an account in geometry bead modelling. Dilution is the amount of base metal which melted and partakes in the structure of the welded component [12]. In order to measure the dilution which occurs on the substrate and first layer of WAAM, the areas which consists of welded component and penetration should be identified and segmented. Depending on parameters used in WAAM process and other variable conditions, a dilution percentage may vary. In this research, an approximately 35% of dilution is occurred within the first layer of WAAM and substrate.



Fig 1: ABB IRB 2400/16 Robotic welding Machine (left) and KEMMPI ProMig 540 MXE (right)

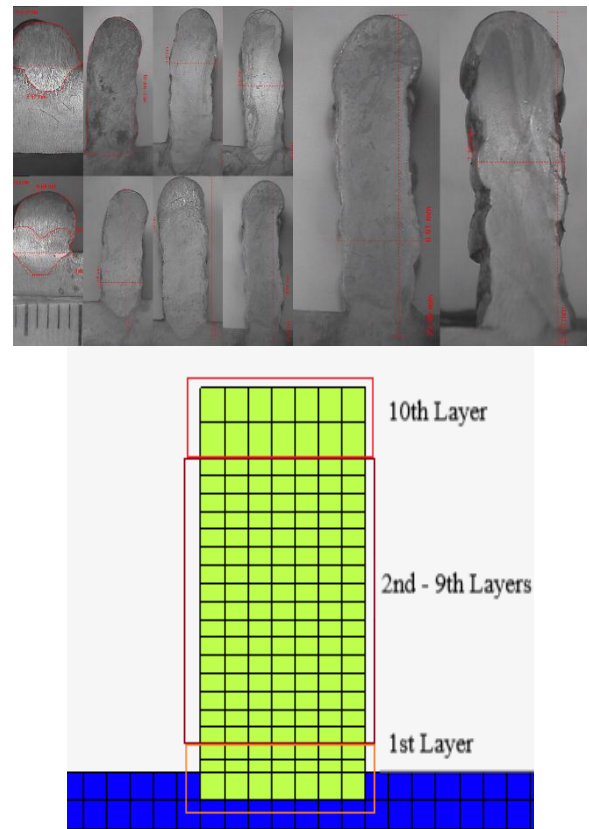


Fig 2: Bead modelling based on macrograph: Macrograph result for each layer of WAAM metal components (Upper) and 10 Layer WAAM bead modelling based on macrograph result (Bottom)

3. Simulation using Nonlinear FEM Software

Analysis for this research in which concerns about distortion of WAAM is executed by means of two-step approaches: FEM simulation and Experimental study. For FEM study, MSC Marc/Mentat is utilized as the sole FEM-based program to conduct a simulation of WAAM process. Procedure of WAAM simulation using MSC Marc/Mentat is demonstrated by Figure 3.

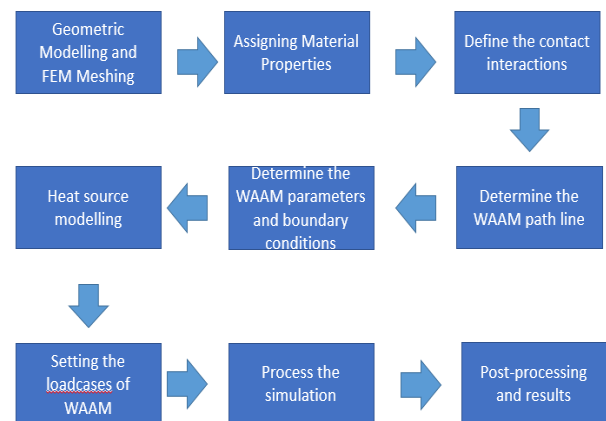


Fig 3: WAAM simulation procedure using MSC Marc/Mentat

WAAM Simulation is based on multi-layered welding which means a bead modelling until boundary conditions procedure is repeated until the number of layers of WAAM model is fulfilled. This research implements a ten layers WAAM beads which means that geometrical bead modelling until boundary conditions step are constantly repeated prior entering the load case setting

3.1 Geometrical and Material Description

On geometrical modelling, a substrate is modelled with dimension of 200 mm x 50 mm x 6 mm which similar to actual Low Carbon Steel substrate that utilized in experimental process. A rectangular-shaped model with 160mm of length along with \varnothing 1.2mm is modelled as filler and consistently sketched from the first layer until the very top.

The basic FEM model along with its bead modelling for this multi-layer WAAM is exhibited in Figure 4. The weld dilution which displayed by macrograph is a crucial factor on determining the weld bead dimension during geometrical modelling. On meshing, each zone is discretized by means of hexahedral elements in uniform mesh.

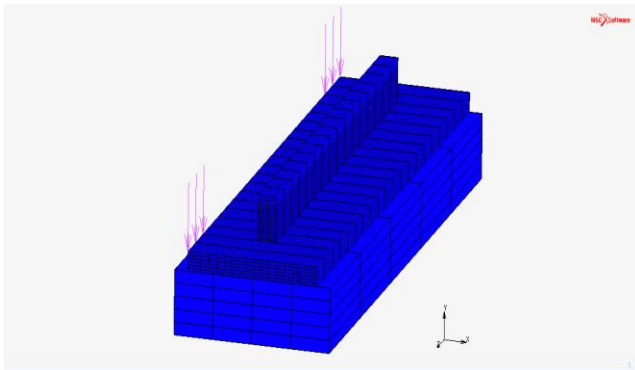


Fig 4: Finite element model of 10 layers WAAM displayed by MSC Marc/Mentat

This simulation assigns High Strength Low Alloy Steel (HSLA) type of material as both filler and Low carbon steel substrate material. In general usage, High strength low alloy (ER80S-Ni) steels have been widely used in pipelines, power plant components, civil structures and so on, due to their outstanding mechanical properties as high strength and toughness [13]. In this simulation, ER80 is chosen as filler material with S235 is assigned as substrate material. Both physicals properties are imported into FEM simulation using the existing databases from previous research, Figure 5 displays the temperature dependant material properties for ER80 and S235 using a material database which are imported into FEM Simulation [14].

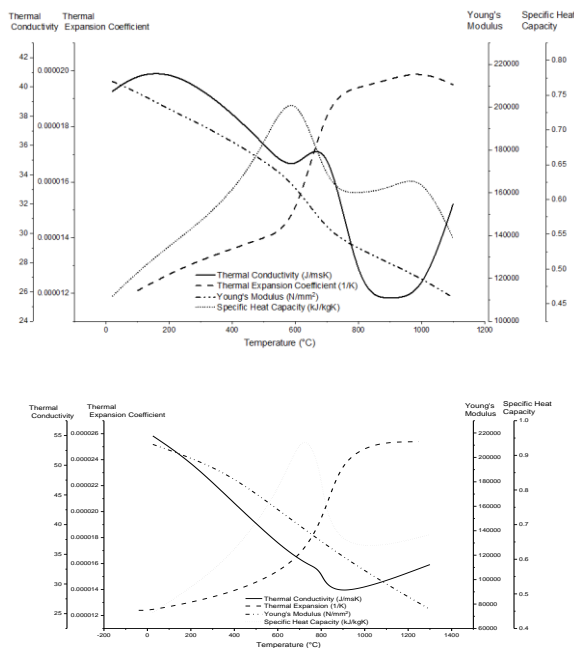


Fig 5: Temperature-dependant thermo-physical properties of ER80s (bottom) and S235 (top)

Previous researches [15-16] had put plasticity analysis within material model into an account in order to investigate the residual stresses on welded component. In this simulative investigation, material behavior model was based on the simplified Hensel-Spittel Model 1 (HS1) as discussed in [17]. The applied constitutive Equation 1 in the simulation is given as:

$$\sigma = A \cdot e^{m_1 \cdot T} \cdot \varphi^{m_2} \cdot e^{\frac{m_4}{\varphi}} \cdot \dot{\varphi}^{m_3} \quad (1)$$

Definition 3.1: A, T, m are scaling factor, temperature and material's sensitivity to temperature (1), strain (2 & 4) and strain rate (3) respectively. The values of the parameters used for the HS1 model equation are as shown in Table 2 below:

Table 2: Values of the parameters used for the HS1 model

Parameter	A	m_1	m_2	m_3	m_4
Value	921.781	-0.0012	0.11291	0.0186	-0.0106
Temperature (T)	20°C – 300°C				
Strain (φ)	0.05 – 2.0				
Strain rate ($\dot{\varphi}$)	0.01s ⁻¹ – 250.0s ⁻¹				

3.2. Process Parameters for FEM Simulations

Parameters which are assigned on MSC Marc/Mentat are shown in Table 3. The Current (I) and the Voltage (V) are considered under the equation of power in MSC Marc/Mentat. Latent heat, solidus and liquidus temperature are adjusted according to actual thermal properties of HSLA material data and they are instigated under material properties section of MSC Marc/Mentat.

Table 3: WAAM parameters used in MSC Marc WAAM simulation

WAAM Parameter	Value
Current, I (A)	100
Voltage, V (V)	16
Travel Speed, v (mm/s)	4

3.3 Heat Source Modelling of FEM Simulation

The state of the art of WAAM is represented by the Goldak's double ellipsoid heat source model, Goldak's double ellipsoid, which is an offered heat source model advocates the heat input as a function to generate heat while also able to control the amount of overall power delivered into substrate and filler [16]. In this model the heat input is delivered over a moving double ellipsoid region according to a Gaussian distribution. Despite such strategy permits to correctly model the shape of the weld pool, it does not take into account the correct heat distribution between filler and base material. Figure 6 displays Goldak's double ellipsoid heat source model.

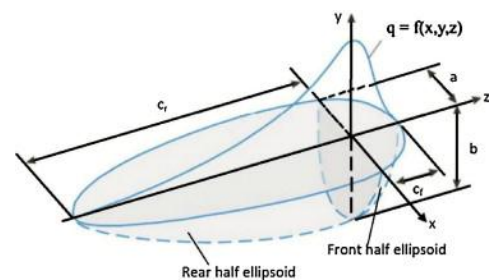


Fig 6: Illustration of Goldak's Double Ellipsoid Heat Source Model

The values for each direction used in WAAM simulation are shown in Table 4, the dimensions are differed depending on the size of the weld bead.

Table 4: Heat Source Dimension in Simulation

Heat Source dimensions	Value (Small bead)	Value (Large bead)
Width (mm)	4	5
Depth (mm)	3.2	5.3
Rear Length (mm)	2.4	3.5
Front Length (mm)	2.4	3.5

4. Result and Discussions

The experimental result of WAAM can be seen in figure 8 below which also states the distortion based on 3 points on the top of a substrate. The visualization set in MSC Marc/Mentat is Contour

Band setting view and its applied for both shell and solid model. Figure 7 exhibits a contour band model which processed by MSC Marc/Mentat on displaying the displacement result of FEM simulation. By looking at FEM result picture, the distribution of stress on the substrate can be examined through the deformed shape and colours in a weld specimen.

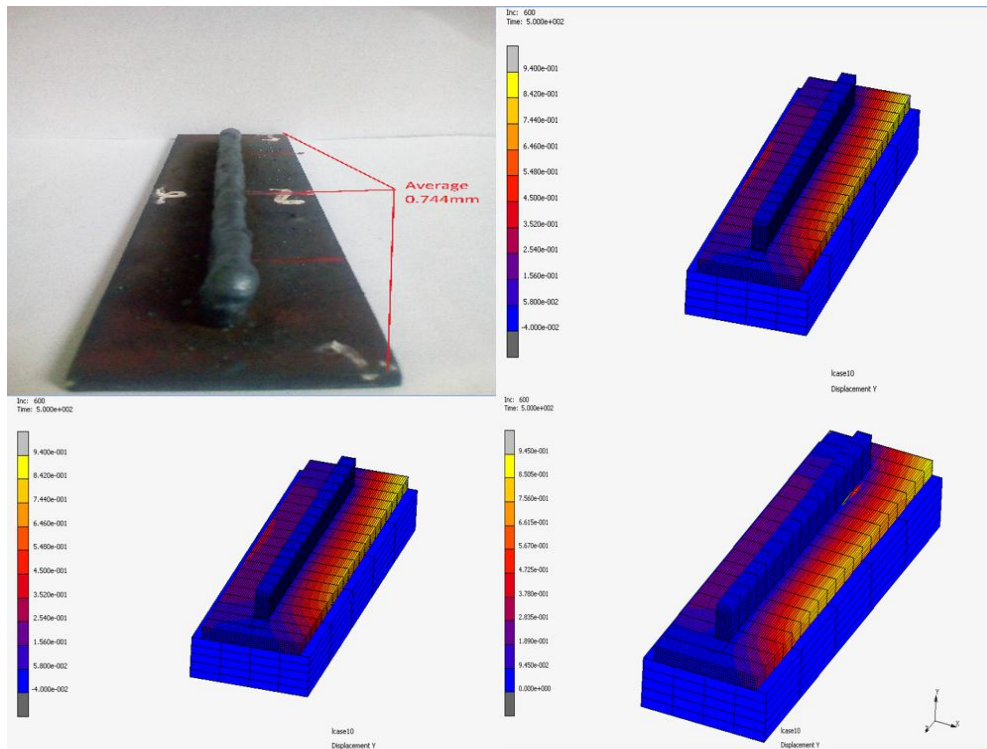


Fig 7: Distortion result displayed by experimental process (Top left) FEM without plasticity model (Top right), FEM with MSC Marc/Mentat default plasticity model (Top left) and FEM with S235 and S460 plasticity model

By looking at these pictures, the distribution of displacements on the weldment surface can be examined through the contour shape and colors in a weld specimen. The table acts as the fixed displacement on both x and z axis under the plate which determines the bearing condition of the weldment and its applied for both simulations. The number that were gathered for the experiment result are from the measurement machine (CMM). By utilizing CMM, the percentage of distortion in certain nodes were calculated, the same nodes also pointed in the FEM simulation.

Three points are selected as a tracking points for measurement of which the average value of the three distortions value will serve the benchmark of comparison. A time-based distortion graph by utilizing history plot on FEM post processing is demonstrated within Figure 9. The distribution of displacement can be examined by the contour band display on the top of substrate, the table is modelled in order to match the real WAAM process and serves as a bottom fixed displacement, clamping condition which implemented here mirrors the actual clamping condition of which a left part of substrate is clamped on 2 points. Distortion of experimental process is the average value of three measurement points which was examined by utilizing the coordinate measurement machine (CMM) on determining the value of distorted region. The exact same areas also measured on post-processing phase in FEM simulation and would be later compared to the distortion result of experiment.

Table 5 exhibits the differences value in distortions resulted in substrate between experimental result and FEM simulation results along with their respective relative error percentage against experimental result. The FEM model involved here consists of WAAM simulation with plasticity effect activated and without plasticity effects.

Table 5: Distortion results of experimental process and FEM simulation

Model	Distortions (mm)			Average distortion (mm)	Relative error percentage (%)
	Point 1	Point 2	Point 3		
Experiment	0.85	0.71	0.67	0.743	-
FEM with MSC Marc/Mentat with Plasticity model of C15	0.96	0.17	0.76	0.63	14.8
FEM with Plasticity model of S235 and S460	0.93	0.21	0.84	0.66	11.1
FEM without Plasticity model	0.47	0.21	0.83	0.51	31.8

5. Conclusion

A fundamental research of Wire Arc Additive Manufacturing which involves both experiment and FEM studies had been executed. The aim is to measure the distortion on metal component substrate by FEM model which modelled after experimental metal component. All parameters, dimension and boundary conditions were set in a similar manner to ensure the similarity between experiment and FEM. In order to conclude this research, some important points of this research are summarized by following statements:

1. Experimental study for 10 layers WAAM produces the results of satisfying weld beads which indicates the assigned parameters well suited to WAAM experiment,
2. FEM of WAAM model which is done using MSC Marc/Mentat was executed successfully of which the procedure is proven to be well structured. FEM Model which

is based on experiment has been proven that it is possible to assign such model in a comprehensive FEM-based WAAM simulation,

3. The distortion results which displayed by FEM shows a good agreement with the experiment result,
4. The FEM simulation with plasticity model displays a better distortion results and exhibits a lower error percentage compared to FEM without plasticity Model,
5. FEM model which assigns the plasticity model for both S235 and S460 display the best result out of 3 simulations,
6. The difference of distortion value between the FEM and experiment might be caused by a non-homogenous material properties along with pre-condition of WAAM process.

As further recommendation, a rectangular heat source model should be taken into account in FEM simulation in order to achieve much better result in overall.

Acknowledgement

The internationally collaborating authors would like to express their gratitude to Advanced Manufacturing Technology Excellence Centre (AMTE_x) and Research Interest Group: Advanced Manufacturing Technology (RIG:AMT) at Faculty of Mechanical Engineering, Universiti Teknologi MARA (UiTM) as well as Professorship Virtual Production Engineering at Chemnitz University of Technology in Germany for providing software and equipment. This research is financially supported by international research grant of DAAD (Ref. Nr.: 57347629) and Geran Inisiatif Penyelidikan (GIP) from Phase 1/2016 with Project Code: 600-IRMI/GIP 5/3 (0019/2016).

References

- [1] Yong ZL, Yunfei S, Qinglin H, Guanjung Z, Imre H, "Enhanced beads overlapping model for wired arc additive manufacturing of multi-layered bead metallic parts", *Journals of Material Processing Tech*, Vol 252 (2018), pp:838-844.
- [2] F. Wang, S. Williams, M. Rush, "Morphology investigation on direct current pulsed gas tungsten arc welded additive layer manufactured Ti6Al4V Alloy". *International Journal Advanced Manufacturing Technology*, Vol 57 (2011), pp:597-603.
- [3] J. Xiong, R. Li, H. Chem, "Heat propagation of circular thin-walled parts fabricated in additive manufacturing using gas metal arc welding". *Journal of Material Processing Technology*, Vol 251 (2018), pp:12-19.
- [4] D. Yang, G. Zhang, "Deposition time and thermal cycles of fabricating thin-wall steel parts by double electrode GMAW based additive manufacturing", *MATEC Web of Conferences* (2017), 88, 01007.
- [5] J.R.R Honnige, P.A. Colegrove, S. Ganguly, E. Eimer, S. Kabra, S. Williams, et al, "Control of residual stress and distortion in aluminium wire + arc additive manufacturing with rolling", *Additive Manufacturing*, Vol 22 (2018).
- [6] G. Venturini, F. Montevercchi, A. Scippa, G. Campatelli, "Optimization of WAAM deposition patterns for T-crossing features", *Procedia CIRP*, Vol 55 (2016), pp:95-100.
- [7] E.R Denlinger, P. Michaleris, "Effect of stress relaxation on distortion in additive manufacturing process", *Additive Manufacturing*, Vol 12a (2016), pp:51-59
- [8] G. Tham, N.F Mohammad Nor, M. Faruqi, J. Saedon, "Prediction of weld bead geometry for small-wire submerged arc welding in 1G position", *Journal of Mechanical Engineering*, Vol 3(2) (2017), pp:145-156
- [9] Z. Hu, X. Qin, T. Shao, "Welding thermal simulation and metallurgical characteristic analysis in WAAM for 5CrNiMo hot forging die remanufacturing", *Procedia Engineering*, Vol 207 (2017), pp:2203-2208.
- [10] J. Francis, H. Stone, S. Kundu, R. Rogge, H. Bhadesdhia, Et al. Transformation temperatures and welding residual stresses in ferritic steels", *ASME 2007 American Society of Mechanical Engineers* (2007), pp: 949-956.
- [11] H. Dai, J. Francis, et al "Characterizing phase transformation and their effects on ferritic weld residual stresses with x-rays and neutrons", *Metalurgical and Material Transaction, Vol 39A* (2008), pp:3070-3078.
- [12] Pedro P.R Filho, T.S Cavalcante, V.H Costa De Alburquerque, P.C Cortez, "Measurement of welding dilution from images using active contours", *Conference Paper* (2009).
- [13] D. Andud, N. Nurdin, Y.H.P. Manurung, M.Faiz M, S. Saidin, "Parameters Identification for Weld Quality, Strength and Fatigue Life Enhancement on HSLA (2460G2+M) using Manual GMAW followed by HFMI/PIT", *Journals of Mechanical Engineering*, Vol S15-4 (2018).
- [14] Y.H.P Manurung, "Database of Common Material Properties", *Unpublished* (2015).
- [15] W. Jiang, W. Chen, W. Woo, Et All, "Effects on low-temperature and transformation-induced plasticity on weld residual stresses: Numerical study and neutron diffraction measurement", *Materials and Design*, Vol 147 (2018), pp:65-79.
- [16] C. Pandey, M.M Mahapatra, P. Kumar, "A comparative study of transverse shrinkage stresses and residual stresses in p91 welded pipe including plasticity error", *Archives of Civil and Mechanical Engineering*, Vol 18 Issue 3 (2018), pp:1000-1011.
- [17] Montevercchi, G. Venturini, A. Scippa, G. Campatelli, "Finite Element Modelling of Wire-arc-additive-manufacturing process", *Procedia CIRP*, Vol 55 (2016), pp:109-114.